

MULTIFREQUENCY NANOMECHANICAL MASS SPECTROMETER PROTOTYPE FOR MEASURING VIRAL PARTICLES USING OPTOMECHANICAL DISK RESONATORS

Oscar Malvar^{1*}, Eduardo Gil-Santos¹, Jose J. Ruz¹, Elena Sentre-Arribas¹, Adrián Sanz-Jiménez¹, Priscila M. Kosaka¹, Sergio García-López¹, Álvaro San Paulo¹, Samantha Sbarra², Louis Waquier², Ivan Favero², Maurits van der Heiden³, Robert K. Altmann³, Dimitris Papanastasiou⁴, Diamantis Kounadis⁴, Ilias Panagiotopoulos⁴, Jesús Mingorance⁵, María Rodríguez-Tejedor⁵, Rafael Delgado⁶, Montserrat Calleja¹ and Javier Tamayo¹

¹Bionanomechanics Lab., Instituto de Micro y Nanotecnología, IMN-CSIC, CSIC (CEI UAM+CSIC), 28760, Tres Cantos, Madrid, SPAIN

²Matériaux et Phénomènes Quantiques, Université Paris Cité, CNRS, UMR 7162, 75013, Paris, FRANCE

³The Netherland Organization for Applied Scientific Research, TNO, NETHERLANDS

⁴Fasmatech Science and Technology, Athens, GREECE

⁵Hospital Universitario La Paz, Madrid, SPAIN and

⁶Hospital Universitario 12 de Octubre, Madrid, SPAIN

ABSTRACT

Nanomechanical mass spectrometry allows characterization of analytes with broad mass range, from small proteins to bacterial cells, and with unprecedented mass sensitivity. In this work, we show a novel multifrequency nanomechanical mass spectrometer prototype designed for focusing, guiding and soft-landing of nanoparticles and viral particles on a nanomechanical resonator surface placed in vacuum. The system is compatible with optomechanical disk resonators, with an integrated optomechanical transduction method, and with the laser beam deflection technique for the measurement of the vibrations of microcantilever resonators. The prototype allows the in-vacuum alignment of resonators thanks to a dedicated visualization system. Finally, in this work, we have demonstrated the detection of gold nanoparticles, polystyrene nanoparticles and phage G viruses with optomechanical disks and microcantilever resonators.

KEYWORDS

Nanomechanical mass spectrometry, optomechanical disk resonators, microcantilevers, mass sensing.

INTRODUCTION

State of the art

Conventional mass spectrometry can measure the mass to charge ratio of small analytes with unprecedented sensitivity, reaching the 18 MDa limit measuring the mass of the bacteriophage HK97 [1]. On the other hand, charge detection mass spectrometry (CDMS) has moved into the mainstream for measuring mass distributions above the MDa regime [2], [3]. However, these technologies need the ionization of the particles and its mass sensitivity degrades for larger analytes. Since the invention of the first nanomechanical mass spectrometer (NMS) system in 2009 in Caltech by Michael Lee Roukes's group [4] this promising technology has demonstrated its potential by measuring the mass of proteins [5], viruses [6] and even bacterial cells [7]. NMS allows weighing individual

particles in real time with outstanding mass sensitivity and with high dynamic range. Furthermore, NMS has demonstrated the measurement of bacteria cell stiffness [8] and even the possibility to extract information of the analyte's shape [9]. Contrary to conventional mass spectrometry or CDMS, NMS doesn't need the ionization of the particles [10], therefore this technique can be used to measure the mass of particles that cannot be ionized, opening the door to new possibilities.

On the other hand, optomechanical resonators present an extraordinary displacement sensitivity, high quality factor together with small masses and high mechanical frequencies, emerging as promising sensors in the nanomechanical spectrometry field [11], [12]. Recently, optomechanical devices have been used in a nanomechanical spectrometer as a sensor element, measuring the mass of tantalum clusters [13]. Moreover, optomechanical disk resonators have proven the detection of vibration modes of a single bacterium [14] and the characterization of the mass of polystyrene nanoparticles in air [15].

Here, we present a multifrequency NMS prototype designed to measure optomechanical disk resonators in vacuum and compatible with the beam deflection technique, for the characterization of nanoparticles and viral particles.

DESCRIPTION OF THE SYSTEM

Nanomechanical mass spectrometer prototype

Figure 1a shows a picture of the multifrequency NMS prototype designed to measure the mass of individual analytes. The prototype is designed for soft-landing, guiding and focusing of the particles on a reduced area by an in-vacuum optical alignment system. The prototype comprises four stages with decreasing pressure. The first stage is at atmospheric pressure and it holds an electrospray ionization (ESI) system for the nebulization of the particles in a controlled atmosphere (Figure 1b), thus avoiding that undesirable particles present in the air can go inside the

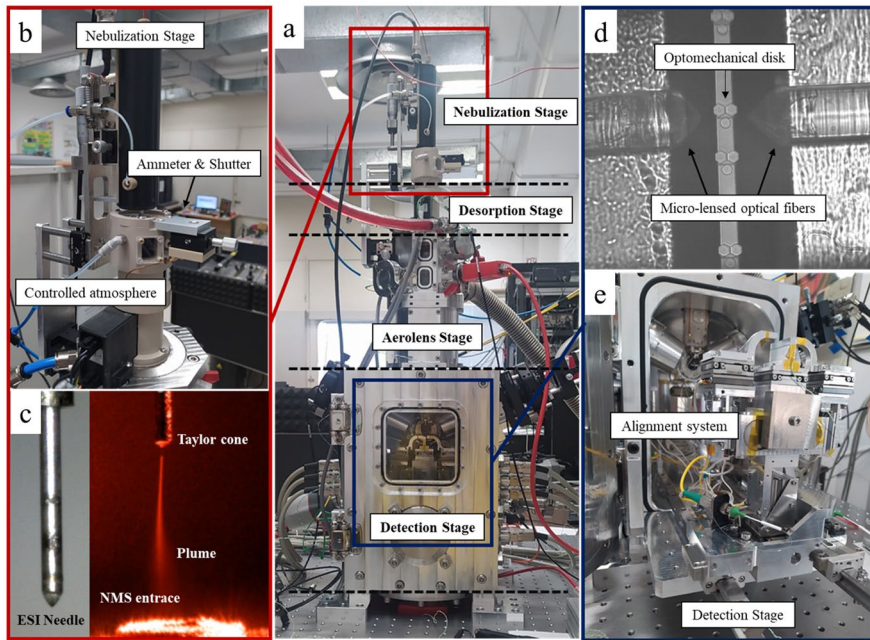


Figure 1: (a) Picture of the nanomechanical mass spectrometer prototype where the four stages with decreasing pressure are shown. (b) Nebulization stage with a controlled atmosphere that contains the ESI system. An ammeter is used to check the stability of the nebulization process and a shutter is used to close or open the system. (c) Picture of the ESI needle used in this work (left) and microscope image showing the Taylor cone and the subsequent expansion plume (right) during the nebulization process. (d) Microscope image of the optomechanical disk resonators taken with the in-vacuum visualization system. (e) Picture of the detection stage where the high precision alignment system is shown.

system and interfering the measurements. An ammeter is used to control the stabilization of the nebulization process measuring the current intensity of the ESI needle with high precision. The ESI nebulization flow rate is set to 0.2 $\mu\text{l}/\text{min}$ by means of a high-pressure syringe pump controller. A sheath and a curtain gas of N_2 is used with a flow rate of 0.3 l/min between the ESI stage and the input of the spectrometer prototype. A high voltage (3–4 kV) is applied to the ESI needle in order to generate the Taylor cone (Figure 1c). A fine jet emerges from tip of the Taylor cone that expand into a plume containing microdroplets with the analytes. The microdroplets evaporate during its way to the next stage to finally have individual particles that can be detected with a nanomechanical sensor element placed in the detection stage. A heated capillary placed at the second stage is set to 200 $^\circ\text{C}$ in order to improve solvent evaporation. Additionally, a water-cooling system isolates this stage to the rest of the prototype in order to reduce thermal effects that can affect the mechanical stability of the system.

The third stage comprises an aerolens designed to reduce the velocity and increase the transportation efficiency of the particles [16]. The resonator element is placed in the fourth stage at 10^{-3} mbar that is designed to measure several resonance frequencies of optomechanical disk or microcantilever resonator by means of an optomechanical transduction method or beam deflection technique, respectively. A designed element focuses the particles in a reduced area of $R = 150 \mu\text{m}$, as measured for 100 nm gold nanoparticles experiments. The prototype also has a visualization/alignment system (Figure 1e) designed to perfectly align the particle beam and the resonator surface and to in-vacuum alignment of the micro-lensed optical fibers and the waveguide integrated into the

optomechanical disk resonator device (Figure 1d) [17]. An automated feedback software continuously tracks the optical transmission in order to maintain the system aligned for long periods of time. The prototype was tested with two different configurations: microcantilever configuration and optomechanical disk resonator set-up.

RESULTS

Microcantilever configuration set-up

The NMS prototype was tested with microcantilever resonators. First, we use a Si_3N_4 microcantilevers array to demonstrate the in-vacuum alignment between the particle beam and the resonator surface. Figure 2a shows a dark field microscope image of an array of 100 microcantilevers and a zoomed image (red dashed circle) showing the nebulization of 100 nm gold nanoparticles. The prototype effectively focuses these particles in a reduced area of around 150 μm of radius with high-efficiency, with a detection of around (12–15) particles per minute. In this experiment, we have tracked the four first flexural modes of a microcantilever with dimensions of 60 μm length, 10 μm width and 100 nm thickness, showed in figure 2a (blue dashed box). Figure 2b shows a real-time record of the relative frequency shifts during the nebulization experiments. After applying the inverse problem algorithm [18], we obtain the mass probability density distribution of these particles.

On the other hand, we have tested the prototype with the nebulization of phage G viral particles. Figure 3a shows the real-time record of the relative frequency shifts of the first three flexural modes during the adsorptions of phage G viral particles on a Si_3N_4 microcantilevers. The dimension of the microcantilever is 40 μm length, 6 μm width and 100 nm thickness. Figure 3b shows the mass

distribution of the viral particles after applying the inverse problem algorithm [18], obtaining a mass distribution between 1 fg and 2 fg, consistent with the expected value, demonstrating the potential of the NMS for viral particles mass sensing using microcantilever resonators.

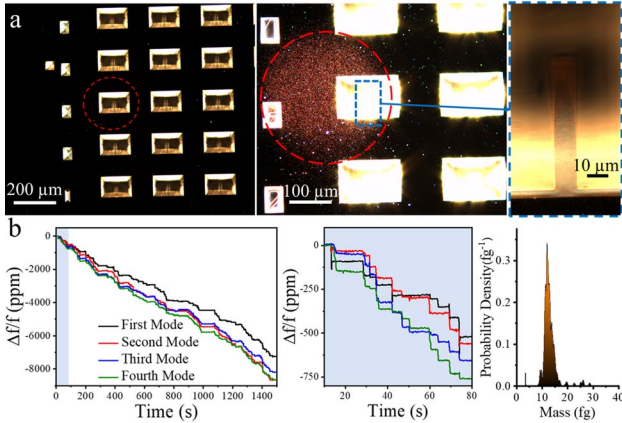


Figure 2: (a) Dark field microscope image of an array of microcantilevers, zoomed image of the nebulized region (red-dashed circle) and microcantilever covered with gold nanoparticles after the experiment (right). (b) Relative frequency shifts of the four tracked modes during the adsorption of 100 nm gold nanoparticles and zoomed area (light-blue). Probability density mass distribution (right) obtained after applying the inverse problem algorithm.

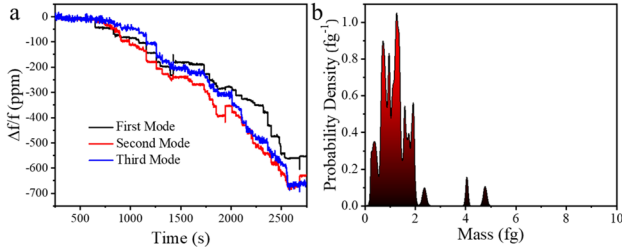


Figure 3: (a) Relative frequency shifts during the phage G experiments on a microcantilever resonator surface. (b) Mass probability density after applying the inverse problem algorithm.

Optomechanical disk resonator set-up

Finally, we have demonstrated the use of 11 μm of radius optomechanical disk resonators as sensor element in the NMS. Figure 4a shows a scanning electron microscope image of an optomechanical disk resonator used in this work. Figure 4b shows the thermomechanical spectrum of the used modes (RBM1, RBM2, M190 and M290) [15] and the simulated modes (inset) given by finite element method (FEM). We have tested the prototype with two different analytes: 140 nm polystyrene nanoparticles (PNPs) and phage G viral particles. Figure 5a shows the relative frequency shifts obtained during a nebulization experiment of 140 nm PNPs. Figure 5b shows the obtained mass distribution and the landing position in polar plot representation of two tentative events after applying the inverse problem algorithm with the optomechanical disk resonators configuration set-up.

On the other hand, Figure 5c shows the real-time record of the relative frequency shifts during the phage G viral particles nebulization experiments. Figure 5d shows

two mass distributions and landing positions in polar plot representation obtained after applying the inverse problem algorithm of two tentative events. The obtained results demonstrate the detection of polystyrene and viral particles with optomechanical disk resonators.

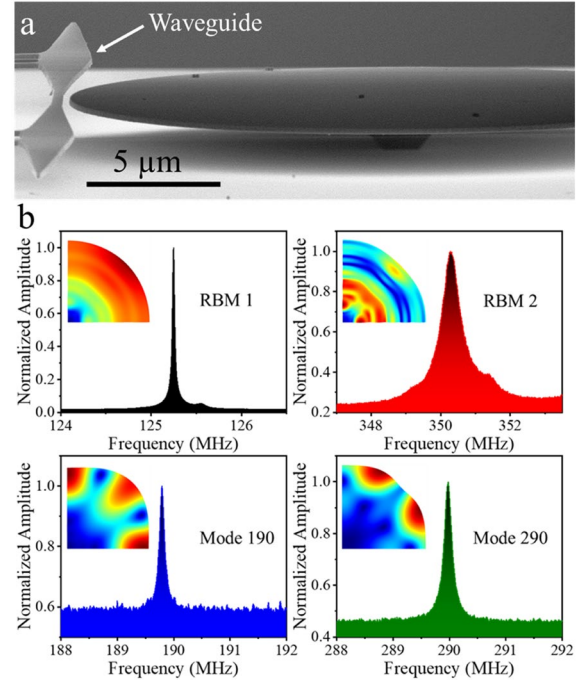


Figure 4: (a) Scanning electron microscope image of an optomechanical disk resonator of 11 μm of radius used in this work. (b) Thermomechanical frequency response of the tracked modes measured in the nanomechanical mass spectrometer prototype. Inset: FEM simulation mode shape representation.

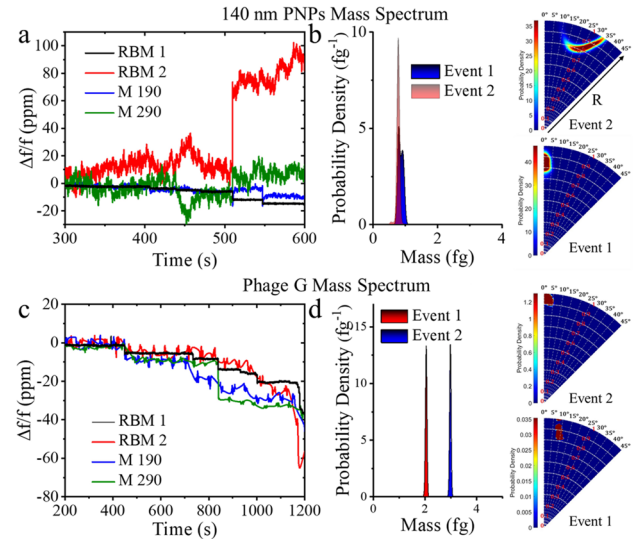


Figure 5: (a) Relative frequency shifts during the nebulization of 140 nm polystyrene nanoparticles. (b) Mass spectrum and landing position in polar plot representation obtained from two tentative events. (c) Relative frequency shift during the nebulization of phage G viral particles. (d) Mass spectrum and landing position in polar plot representation of two tentative events during the nebulization of phage G viral particles.

However, there are two important factors that need to be considered in order to extract the mass and position with more accuracy. First, we need to perfectly know the used mode shapes of the optomechanical disk resonators in order to apply the inverse problem algorithm, what is complicated due to the unknown of the pedestal geometry that modify the expected mode shapes (Figure 4b insets). Second, some of the particle adsorptions could produce a change in the optomechanical coupling or in the optical quality factor, altering the mechanical frequency shifts (like positive frequency shifts observed in Figure 5a) and interfering in the correct mass and position calculations. Despite these undesirable effects, we have obtained mass distribution values of some tentative measured events that are in good agreement with the expected masses, suggesting that optomechanical mass spectrometry can play an important role in the future, with huge applications in the environment or biomedical fields, for instance, in the detection of nanoparticles and microbiological entities.

CONCLUSION

In conclusion, we show here a novel multifrequency nanomechanical mass spectrometer prototype, compatible with microcantilever and with optomechanical disk resonators, that can measure several frequencies at the same time. The prototype is able to nebulize, guide and soft-land nanoparticles and viral particles from solvent solution to the surface of optomechanical disk and microcantilever resonators in vacuum. Finally, we have tested the prototype with gold nanoparticles, polystyrene nanoparticles and phage G viral particles obtaining promising results.

ACKNOWLEDGEMENTS

This work was supported by the European Union's Horizon 2020 Research and Innovation Program under Grant Agreement No. 731868-VIRUSCAN, by the EIC Pathfinder Innovation Council 101034583-H2020 VIRAIR and by the project PCL2021-007892 PTI Salud Global (CSIC). We acknowledge the service from the Micro and Nanofabrication Laboratory and X-SEM laboratory at IMN-CNM funded by the Comunidad de Madrid (Project S2018/NMT-4291 TEC2SPACE) and by MINECO (Project CSIC12-4E-1794 with support from FEDER, FSE). E. G. S. acknowledges financial support by the Spanish Science and Innovation Ministry through Ramón y Cajal grant RYC-2019-026626-1 and by the BBVA Foundation through "Leonardo Grant investigadores y creadores culturales 2021" – DISOM project.

REFERENCES

- [1] J. Snijder, R. J. Rose, D. Veesler, J. E. Johnson, and A. J. R. Heck, "Studying 18 MDa Virus Assemblies with Native Mass Spectrometry," *Angewandte Chemie International Edition*, vol. 52, no. 14, pp. 4020–4023, Apr. 2013.
- [2] D. Z. Keifer, E. E. Pierson, and M. F. Jarrold, "Charge detection mass spectrometry: weighing heavier things," *Analyst*, vol. 142, no. 10, pp. 1654–1671, 2017.
- [3] A. R. Todd, L. F. Barnes, K. Young, A. Zlotnick, and M. F. Jarrold, "Higher Resolution Charge Detection Mass Spectrometry," *Anal. Chem.*, vol. 92, no. 16, pp. 11357–11364, Aug. 2020.
- [4] A. K. Naik, M. S. Hanay, W. K. Hiebert, X. L. Feng, and M. L. Roukes, "Towards single-molecule nanomechanical mass spectrometry," *Nat. Nanotechnol.*, vol. 4, no. 7, pp. 445–450, 2009.
- [5] M. S. Hanay *et al.*, "Single-protein nanomechanical mass spectrometry in real time," *Nat. Nanotechnol.*, vol. 7, no. 9, pp. 602–608, 2012.
- [6] S. Dominguez-Medina *et al.*, "Neutral mass spectrometry of virus capsids above 100 megadaltons with nanomechanical resonators," *Science (1979)*, vol. 362, no. 6417, pp. 918–922, Nov. 2018.
- [7] A. Sanz-Jiménez *et al.*, "High-throughput determination of dry mass of single bacterial cells by ultrathin membrane resonators," *Commun. Biol.*, vol. 5, no. 1, p. 1227, 2022.
- [8] O. Malvar *et al.*, "Mass and stiffness spectrometry of nanoparticles and whole intact bacteria by multimode nanomechanical resonators," *Nat. Commun.*, vol. 7, no. 1, p. 13452, 2016.
- [9] M. S. Hanay, S. I. Kelber, C. D. O'Connell, P. Mulvaney, J. E. Sader, and M. L. Roukes, "Inertial imaging with nanomechanical systems," *Nat. Nanotechnol.*, vol. 10, no. 4, pp. 339–344, 2015.
- [10] E. Sage *et al.*, "Neutral particle mass spectrometry with nanomechanical systems," *Nat. Commun.*, vol. 6, Mar. 2015.
- [11] M. Aspelmeyer, P. Meystre, and K. Schwab, "Quantum optomechanics," *Phys. Today*, vol. 65, no. 7, pp. 29–35, Jul. 2012.
- [12] X. Liu *et al.*, "Progress of optomechanical micro/nano sensors: a review," *Int. J. Optomechatronics*, vol. 15, no. 1, pp. 120–159, Jan. 2021.
- [13] M. Sansa *et al.*, "Optomechanical mass spectrometry," *Nat. Commun.*, vol. 11, no. 1, p. 3781, 2020.
- [14] E. Gil-Santos *et al.*, "Optomechanical detection of vibration modes of a single bacterium," *Nat. Nanotechnol.*, vol. 15, no. 6, pp. 469–474, 2020.
- [15] S. Sbarra, L. Waquier, S. Suffit, A. Lemaître, and I. Favero, "Multimode Optomechanical Weighting of a Single Nanoparticle," *Nano Lett.*, vol. 22, no. 2, pp. 710–715, Jan. 2022.
- [16] D. Papanastasiou *et al.*, "Experimental and numerical investigations of under-expanded gas flows for optimal operation of a novel multipole differential ion mobility filter in the first vacuum-stage of a mass spectrometer," *Int. J. Mass Spectrom.*, vol. 465, p. 116605, Jul. 2021.
- [17] E. Gil-Santos *et al.*, "High-frequency nano-optomechanical disk resonators in liquids," *Nat. Nanotechnol.*, vol. 10, no. 9, pp. 810–816, 2015.
- [18] J. J. Ruz, O. Malvar, E. Gil-Santos, D. Ramos, M. Calleja, and J. Tamayo, "A review on theory and modelling of nanomechanical sensors for biological applications," *Processes*, vol. 9, no. 1, 2021.

CONTACT

*O. Malvar, tel: +34-918060700 (ext. 440858);
oscar.malvar@csic.es